BASIC SCIENCE

Nanomedicine: Nanotechnology, Biology, and Medicine
8 (2012) 1282–1292

nanomedicine
Nanotechnology, Biology, and Medicine

Research Article

nanomedjournal.com

Effects of nanoparticle surface-coupled peptides, functional endgroups, and charge on intracellular distribution and functionality of human primary reticuloendothelial cells

Matthias Bartneck, PhD[a,*], Heidrun A. Keul, PhD[b], Mona Wambach, Dipl-Chem[b], Jörg Bornemann, PhD[c], Uwe Gbureck, PhD[d], Nico Chatain, PhD[e], Sabine Neuss, PhD[f], Frank Tacke, MD, PhD[a], Jürgen Groll, PhD[d], Gabriele Zwadlo-Klarwasser, PhD[g]

[a]*Department of Medicine III, Medical Faculty, RWTH Aachen, Aachen, Germany*
[b]*DWI e.V. and Institute of Technical and Macromolecular Chemistry, RWTH Aachen, Aachen*
[c]*Electron Microscopic Facility (EMF), Medical Faculty, RWTH Aachen, Germany*
[d]*Department and Chair of Functional Materials in Medicine and Dentistry, University of Würzburg, Würzburg, Germany*
[e]*Institute of Biochemistry and Molecular Biology, Medical Faculty, RWTH Aachen, Aachen, Germany*
[f]*Institute of Pathology, Medical Faculty, RWTH Aachen, Aachen, Germany*
[g]*Interdisciplinary Center for Clinical Research and Department of Dermatology, Medical Faculty, RWTH Aachen, Aachen, Germany*

Received 10 October 2011; accepted 22 February 2012

Abstract

The medical use of nanoparticles (NPs) has to consider their interactions with the cells of the reticuloendothelial system. In this study the authors used gold nanorods coated by PEG chains bearing peptides or charged functional groups to study their influence on the uptake, subcellular distribution, and activation of human primary reticuloendothelial cells: monocytes, macrophages (MΦ), immature and mature dendritic cells (DC), and endothelial cells (EC). We found that beside MΦ and immature DC also EC internalize large quantities of NPs and observed an increased uptake of positively charged particles. Most notably, NPs accumulated in the MHC II compartment in mature DC that is involved in antigen processing. Furthermore, surface-coupled peptide sequences RGD and GLF altered the activation profile of DC, and modulated cytokine release in both DC and MΦ in a cell specific manner. These data suggest that the charge of NPs mainly influences their uptake, whereas conjugated peptides alter cell functions.

From the Clinical Editor: In this paper the interactions between RES cells and nanoparticles is investigated, concluding that in the case of gold nanorods charge determines uptake characteristics, whereas conjugated peptides determine their function.

Key words: Dendritic cells; Macrophages; Endothelial cells; Gold nanorods; Peptides

Gold nanoparticles (AuNPs) exhibit a strong absorption in the visible light, rendering them useful for a number of applications, including imaging, optical coherence tomography, dark-field microscopy, computed tomography, and two-photon luminescence.[1] Anisotropic particles such as gold nanorods (AuNRs) further posses a second absorption band that corresponds to the anisotropy of the particles and thus can be tuned in wavelength. We found it most interesting that absorption in the near infrared can be achieved, a wavelength area at which absorption and scattering by human tissue is minimal. This feature and the generation of heat upon nanorod irradiation can be used therapeutically to eradicate tumor cells.[2]

Usually, enrichment of NPs in tumors is facilitated by using the passively acting enhanced permeability and retention (EPR) effect where NPs pass through the more leaky vessels in tumor tissue and accumulate over time. PEGylation of NPs enhances

No conflict of interest was reported by the authors of this paper.

This study was supported by the German Research Foundation research training group "Biointerface" (GRK1035), the BMBF (13N9176 "Nano-SRT"), the EU (FP 6, IP NanoBio-Pharmaceutics), the Interdisciplinary Centre for Clinical Research (IZKF Aachen) within the faculty of Medicine at the RWTH Aachen, and the German Research Foundation (DFG Ta434/2-1).

*Corresponding author: Department of Medicine III, Medical Faculty, RWTH Aachen, Pauwelsstr. 30, Aachen 52074, Germany.
E-mail address: mbartneck@ukaachen.de (M. Bartneck).

1549-9634/$ – see front matter © 2012 Elsevier Inc. All rights reserved.
http://dx.doi.org/10.1016/j.nano.2012.02.012

the blood circulation time by minimizing interactions of NPs with immune cells[3] and hence enables accumulation of NPs in tumor tissue by the EPR effect.[4] However, the penetration into solid tumors is strongly reduced without additional targeting moieties on the NP surface.[5,6] This penetration can be improved by presenting biologically active peptides on the NP surface, such as the arginine-glycine-aspartic acid (RGD) tripeptide that binds to tumor cells due to their enhanced expression of integrin[6,7] or of Herceptin, a monoclonal antibody that enables targeting of breast cancer cells.[8] It remains to be clarified how the addition of such moieties affects the interaction with cells of the innate immune system and, in addition, with the endothelial cells that flank the blood vessels.[9,10]

Professional phagocytes and endothelial cells represent the reticuloendothelial system (RES). Monocytes are the common progenitor of macrophages (MΦ) and dendritic cells (DC). Their path of differentiation is defined by a large number of mediators such as cytokines, glucocorticoids (that induce alternative activation of MΦ), microbial stimuli (leading to classical activation), and specific cytokines (such as the granulocyte-macrophage colony-stimulating-factor, GM-CSF and interleukin IL-4) that promote differentiation of monocytes into DC.[11]

DCs significantly enhance the activities of their peptide-degrading enzymes for antigen presentation by tightly controlling the pH level of the proteasome.[12,13] Proteases facilitate a rapid peptide-bond cleavage, acting as highly efficient catalysts and facilitating hydrolysis of peptide unions within milliseconds.[14] In addition to an enhanced expression of human leukocyte antigen (HLA), DC maturation is also accompanied by increased expression levels of co-stimulatory molecules, such as CD80, CD83, and CD86, that enhance binding of the MHC II complex to the T cell receptor.[15] Immature DC, such as Langerhans cells, express high levels of CD1a,[16] a glycoprotein belonging to the group one of CD1 proteins that share the capacity to present microbial lipid antigens to T cells. The typical phenotype of human DC is $CD1a^{+}$ $CD14^{-}$, whereas that of MΦ is $CD1a^{-}$ $CD14^{+}$.[17] CD14 is a receptor for complexes of bacterial products such as lipopolysaccharides (LPS) and the LPS- binding protein.[18]

We have recently demonstrated that the inflammatory response of human MΦ is strongly affected after 1 week of incubation with AuNRs, depending on charged functional groups presented on the NP surface.[9] Others have shown that NP-encapsulated peptides affect DC maturation and cell-stimulatory capacity,[10] but a direct comparison between the effects of charge and peptide-coupled NRs has not yet been performed. In addition, a combined study of MΦ and DC regarding their interactions with NPs has not been conducted until now and could contribute to a better understanding of the functional differences between these closely related cell types.

In this study, we focused on AuNPs, spherical and rod shaped, that were modified with functional polyethylene glycol (PEG) chains bearing negatively and positively charged functional groups as well as the tripeptides arginine-glycine-aspartic acid (RGD) and glycine-leucine-phenylalanine (GLF), which exhibit different biological functions. The RGD motif originates from fibronectin and is known to initiate the binding of extracellular matrix proteins such as fibronectin and of laminin to integrins.[7] The GLF peptide was reported to be macrophage-binding.[19] We studied the uptake of these particles by six different types of human primary RES cells. Further, we compared the response of DC and MΦ after 48 hours of stimulation with AuNRs stabilized with cetyl-trimethylammoniumbromide (CTAB), PEG-OH, PEG-NH_2 and PEG–COOH, as well as with the particle-coupled peptides PEG-RGD and PEG-GLF. The cellular response of DC and MΦ following long-term culture of 48 hours was characterized on the level of function-associated surface marker expression and by measuring the release of 13 cytokines.

Methods

Materials

Tetrachloroauric(III)acid monohydrate (≈52% Au), N-hydroxysuccinimide (NHS), and CTAB were obtained from Fluka (Buchs, Switzerland). Silvernitrate, L-(+) ascorbic acid, sodium borohydride, hydroxylamine (50 wt% in water) and 1-ethyl-3-(dimethylaminopropyl)-carbodiimide (EDC) were purchased from Sigma-Aldrich (St. Louis, Missouri) and 2-(N-morpholino)ethane sulfonic acid (MES) from Merck (Darmstadt, Germany). PEG polymers used were obtained from Iris Biotech (Marktredwitz, Germany), and the amino acid sequences GRGDS-NH_2·CF_3COOH, and GLF-NH_2·CF_3COOH from Bachem (Weil am Rhein, Germany). Ortho-phthaldialdehyde (OPA) was obtained from Agilent (Agilent Technologies, Santa Clara, California). For all syntheses deionized water was used and was obtained from an Elga Purelab Ultra Plus UV (ELGA LabWater, L'Aquarène, France). Citrate stabilized spherical gold colloids were acquired from Aurion (Wageningen, The Netherlands) (d = 15 nm), and green fluorescent silica-based nanospheres (d = 50 nm) were obtained from Micromod (Rostock-Warnemuende, Germany).

NP preparation

The ligand exchange of citrate stabilized 15 nm nanospheres with CTAB was done as shown before.[9] Gold nanorods (50 × 15 nm) were prepared via a seed-mediated growth procedure[20] and the ligand exchange against commercial 3 kDa PEG with alcohol, amino or carboxy groups at the other end of the polymer chain as published earlier.[9] To couple peptides, concentrated carboxy-functionalized AuNR dispersions were diluted with an equal volume of MES buffer (0.10 M MES, 0.51 M NaCl, and 0.039 M NaOH in deionized water, pH 6). Equimolar amounts of EDC and NHS in relation to the fraction of carboxy groups present in the NRcoating were added to the particle solutions to create the corresponding active esters. After 15 minutes of incubation at room temperature (21°C), aqueous solutions of the protected amino acid sequences (GRGDS-NH_2·CF_3COOH or GLF-NH_2·CF_3COOH, 70 mM) were added in the desired molar amounts between 5% and 25% of the total amount of carboxy groups. After 24 hours, remaining active ester groups were quenched by the addition of hydroxyl amine to a final concentration of 10 mM. Purification was done by centrifugation (11,000 rcf, 10 minutes).

NP characterization

A UV-Vis spectrophotometer UV160A (Shimadzu, Tokio, Japan) was used for aquiring optical spectra. Zeta potential measurements were performed on a Zetasizer Nano ZS (Malvern Instruments, Malvern, United Kingdom). Transmission electron microscopy (TEM) images of NPs were taken with a Libra 120 TEM (Zeiss, Oberkochen, Germany) with an accelerating voltage of 120 kV. Contaminations of NP dispersions with bacteria were excluded due to endotoxin testing as reported earlier.[9]

An Agilent 1100 HPLC equipped with an autosampler, and a fluorescence detector of the Agilent 1200 series was used for semi-quantitative analysis of free and NP-coupled peptides based on their peak areas in HPLC. Peptide-functionalized AuNR were fluorescently labeled with OPA according to the instructions of the manufacturer (Agilent Technologies). Measurements were performed at 40°C with an Eclipse Plus C18 column at a flow rate of 2 mL/minute. As solvent system, a phosphate borate buffer at pH 8.2 (19 mM sodium borate, 5 mM Na_2HPO_4, 15 mM NaN_3 in filtrated/degassed water) and an acetonitrile/methanol/water mixture (v/v/v: 45/45/10) was used. For both amino acid sequences a gradient method was done according to the instructions of the manufacturer (Agilent Technologies). GLF was excitated at 240 nm, and the emission was recorded at 280 nm. RGD was excitated at 230 nm, and its emission was measured at 450 nm (for further details see Supplementary Information, Section 1, available online at http://www.nanomedjournal.com).

Cell isolation, culture, and treatment with NPs

Monocytes were obtained from blood of single human donor buffy coats (Institut für Transfusionsmedizin, Universitätsklinikum Aachen, Germany) by purification of peripheral blood mononuclear cells (PBMC) using Ficoll Paque density gradient centrifugation (Pharmacia, Erlangen, Germany).[9] Monocytes were isolated from PBMC using the Dynal® Monocyte Negative Isolation Kit (Dynal Biotech, Oslo, Norway).[9] The local Ethical Committee gave ethical approval for this study, and informed consent was obtained from all participants. Endothelial cells were obtained from human umbilical veins by mild proteolytic digestion as described previously.[21] For details about endothelial cell isolation, see Supplementary Information Section 2.

To obtain MΦ, monocytes were isolated as described earlier[9] and were cultured for 7 days at a density of 1 million cells per mL in bacterial grade petri dishes in RPMI1640 medium (Sigma, München, Germany) medium with 5% autologous human serum.[9] For the generation of immature DC, monocytes were cultured in six-well plates at the same cell density supplemented with 2% human serum in the presence of IL4 and GM-CSF (R&D Systems, Minneapolis, Minnesota) for 7 days. Replacement of 1 mL cytokine-containing medium every other day as shown before.[22] Maturation of DC was induced by treating the cells with a cocktail of pro-inflammatory cytokines: interleukin 1β (IL1β), IL6, IL4, granulocyte-macrophage colony stimulating factor (GM-CSF) (R&D Systems), and Prostaglandin E2 (Sigma-Aldrich, München, Germany) as described before.[23]

For uptake studies with MΦ and immature DCs, one million cells were incubated in RPMI1640 medium with 5% human serum (immature DCs additionally received IL4 and GM-CSF) and concentrated NP dispersions were added: 1.19 μg gold/mL AuNR, and 1.25 μg gold/mL of AuNS, respectively. Short-term experiments took 60 minutes, whereas long-term conditions lasted for 48 hours.

Intracellular distribution and quantification of NPs

The enlargement of AuNPs up to the micro-scale was performed using cytospin preparations of the cells and an optimized protocol of the GoldEnhance LM Kit 2112 (Nanoprobes, Yaphank, New York) as described earlier in detail.[9] To prepare cells for TEM, cells were fixed in 3% glutaraldehyde for 22 hours, embedded in 2% agarose, incubated for 1 hour of incubation in 1% osmium tetroxide, rinsed with distilled water, and dehydrated with ethanol and propylenoxide. Preparations were cut into 80-nm-thin sections and analyzed with an EM 400 T (Philips, Amsterdam, The Netherlands) at 60 kV. Micrographs were taken using a CCD-Camera MORADA (Olympus, Tokyo, Japan).

To measure the content of cell-immobilized NPs, cells were dissolved in 1 mL of 37% hydrochloric acid (HCl). After 10 minutes of centrifugation at 3000 *g*, 0.5 mL of the supernatant were diluted with 4.5 mL double-distilled water. After further centrifugation for 10 minutes, the solution was diluted to an equal part with 3.7% HCl. A commercial gold standard solution (Merck, Darmstadt, Germany) was used to quantify the amount of gold using inductively coupled plasma mass spectroscopy (ICP-MS) (Varian, Darmstadt, Germany).

Flow cytometry and fluorescence microscopy

Cell surface antigens of DCs were stained with fluorescently labeled monoclonal antibodies anti-CD1a (clone HI149), anti-CD80 (clone L307.4), anti-CD86 (clone 2331(FUN-1)), and anti-CD14 (clone M5E2). MΦ were stained using anti-CD163 (clone GHI/61) (R&D Systems) and for anti-S100A8/S100A9 using anti-27E10 (BMA Biomedicals AG, Augst, Switzerland). Flow cytometry was performed using a FACSCalibur and the BD CellQuest Pro software version 5.2.1 (Becton Dickinson, Franklin Lakes, New Jersey). Confocal microscopy was done using a Zeiss LSM-710 confocal microscope, and image analysis was performed using the ZEN software (Carl Zeiss, Jena, Germany).

Cytokine detection

The release of 13 cytokines (CCL2, CCL3, CCL4, CSF3, CXCL8, CXCL9, IFNγ, IL1β, IL6, IL10, IL12p70, TNFα and TNFβ) into the culture medium was measured using the FlowCytomix® system in collaboration with the producing company (Bender Medsystems, Vienna, Austria). Measurements were performed in duplicates at 50 μL sample volume.

Statistical analysis

Statistical analysis was performed using Graph Pad Prism 4.0. One-way analysis of variance with Bonferroni's post test was

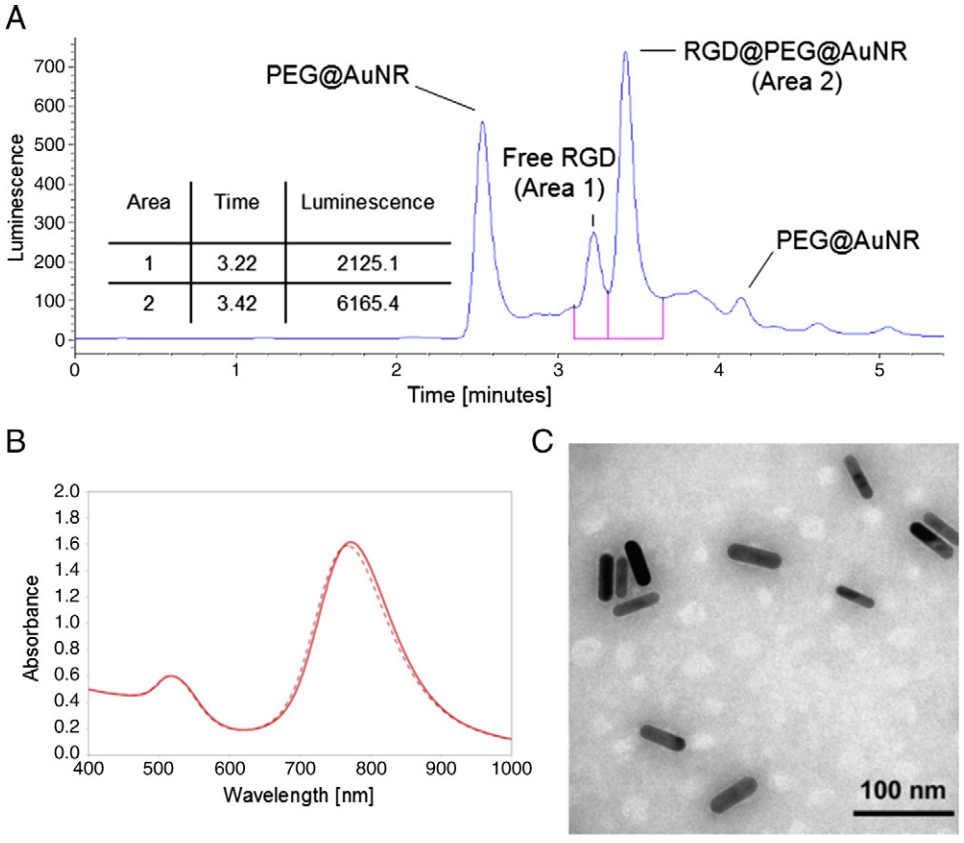

Figure 1. Analysis of the properties of AuNRs after functionalization with peptides. High-pressure liquid chromatography analysis of peptide conjugation onto AuNRs **(A)**. UV-Vis optical characterization of HS-PEG-COOH/OH-modified gold AuNRs before (*continuous line*) and after modification with the RGD peptide (*dashed line*) **(B)**. TEM micrograph of nanorod morphology after coupling with peptides **(C)**.

performed to test significance of data. *P* values below 0.05 were considered statistically significant.

Results

Functionalization of AuNRs

AuNRs were synthesized according to seed-growth mechanisms, and ligand exchange of CTAB against thiofunctional PEG with different functional groups was performed as reported earlier.[9] In addition, two peptide sequences with specific biochemical effects, RGD and GLF, were covalently attached to AuNRs that were coated with mixtures of HS-PEG-COOH and HS-PEG-OH at a ratio of 1:3 using EDC/NHS coupling chemistry. It appeared that 25% of COOH were most efficient to functionalize NRs with these peptides, and therefore, 25% of COOH and 50% OH were used.

Analysis of the biofunctionalized NRs was performed via qualitative HPLC analysis of the fluorescent peptide derivatives. A representative chromatogram of RGD- modified NRs is shown in Figure 1, *A*. The RGD peak was assigned by the measurement of reference samples. Free RGD eluted after slightly shorter retention times than PEG-RGD compounds (Δ = 0.2 minutes) (Figure 1, *A*). UV-Vis spectroscopy revealed that the aspect ratio of the NRs was not affected by the coating procedure as exemplarily shown for RGD-functionalized NRs (in Figure 1, *B*) and TEM proved that the NRs remained stable (Figure 1, *C*). This finding demonstrates successful immobilization of the peptides on the PEG-chains. Details on the HPLC analysis are discussed in Supplementary Information Section 1.

Uptake of NPs by cells of the RES

In the first set of experiments, we investigated whether primary human RES cell populations differ in their uptake of spherical NPs. To that end, we used established protocols[9] and cetyl-trimethylammoniumbromide (CTAB)-capped AuNS of 15-nm diameter at the optimal concentration 1.25 μg gold/mL and incubation time of 60 minutes. Using seedless deposition, we found marked differences concerning the intracellular distribution of the NPs. In mature DC and less pronounced also in MΦ cultured for 3 days, the particles were found to accumulate in distinct spot-like areas (Figure 2, *A*,*E*). In immature DC, MΦ, monocytes and endothelial cells (*B*-*F*), NPs were distributed throughout the whole cell (Figure 2).

To study the role of the NP stabilizer and its corresponding surface charge, we compared the uptake of positively charged CTAB-stabilized nanospheres (zeta-potential of +49.6 mV) with negatively charged citrate-stabilized particles (-39.3 mV).[9] Enumerations based on seedless deposition revealed that more

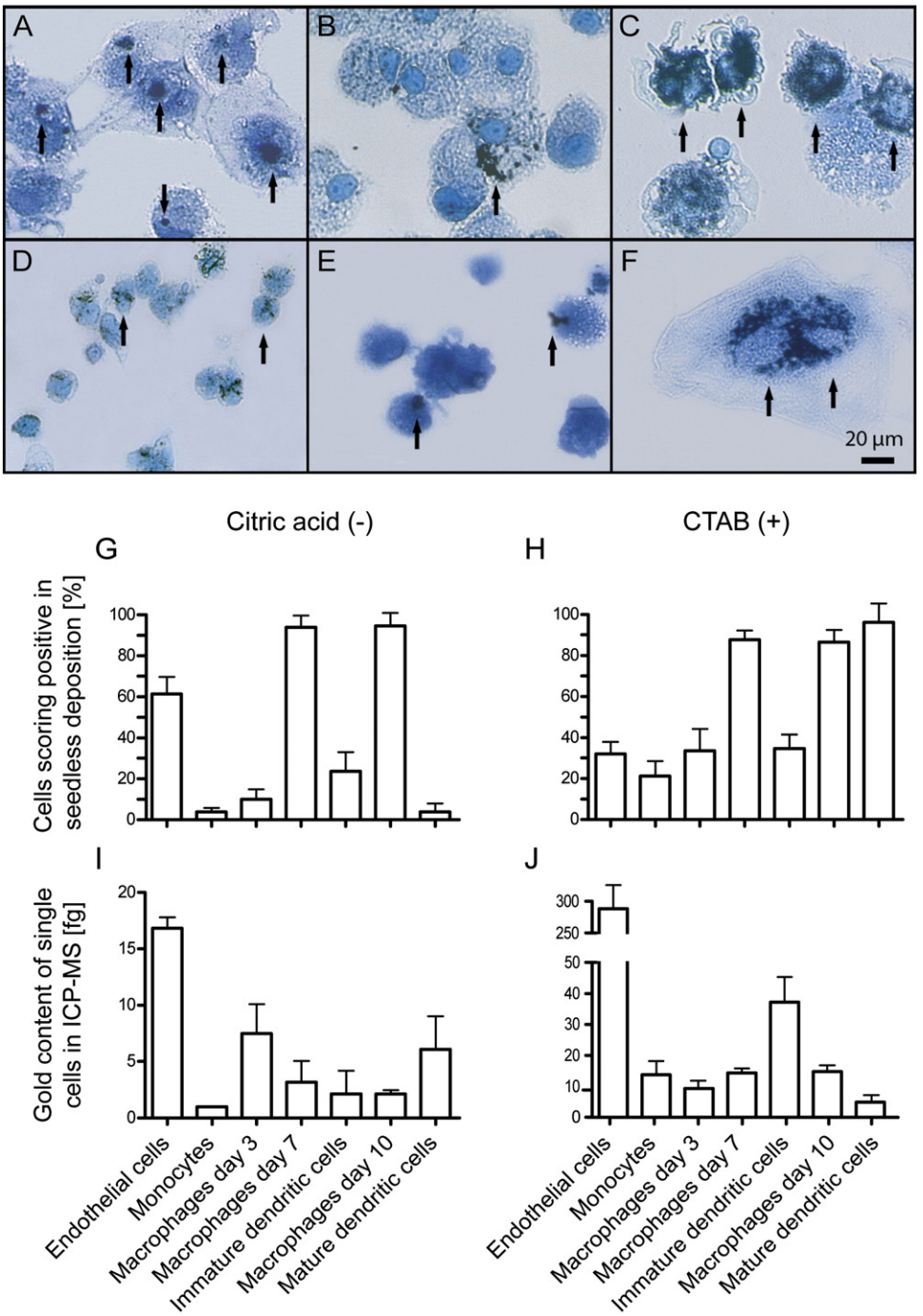

Figure 2. Intracellular distribution and intake of AuNPs by different RES cells. Cytospin preparations after 60 mins of incubation with CTAB-coated Au nanospheres followed by seedless deposition **(A-F)**. Mature dendritic cells **(A)**, immature dendritic cells **(B)**, MΦ day 7 **(C)**, monocytes **(D)**, MΦ at day 3 **(E)**, and endothelial cells **(F)** after 60 mins of incubation with CTAB-coated Au nanospheres. Black arrows point at the size-enhanced AuNPs. Quantitative display of the effect of NP stabilizer charge (citrate or CTAB) on the percent positive cells based on seedless deposition **(G,H)** and of cellular intake per cell measured by ICP-MS **(I,J)**. Data represent mean values and standard deviation (SD) (n = 6).

than 61% of endothelial cells and 95% of mature MΦ scored positive for the uptake of citric-acid-stabilized NPs, whereas only 4% of monocytes, 24% of immature DC, and 3.8% of mature DC were positive. Notably, replacement of citrate (Figure 2, *G*) with CTAB strongly increased the portions of cells containing NPs in particular in mature DCs (Figure 2, *H*).

An ICP-MS-based quantification of the cellular content of NPs showed that endothelial cells internalized large amounts of citric acid-stabilized NPs. Further, we found that the MΦ of day 3 and mature DC internalized the second largest quantities of gold (I). The increased uptake of positively charged particles by all cells was confirmed by ICP-MS and remarkably, endothelial

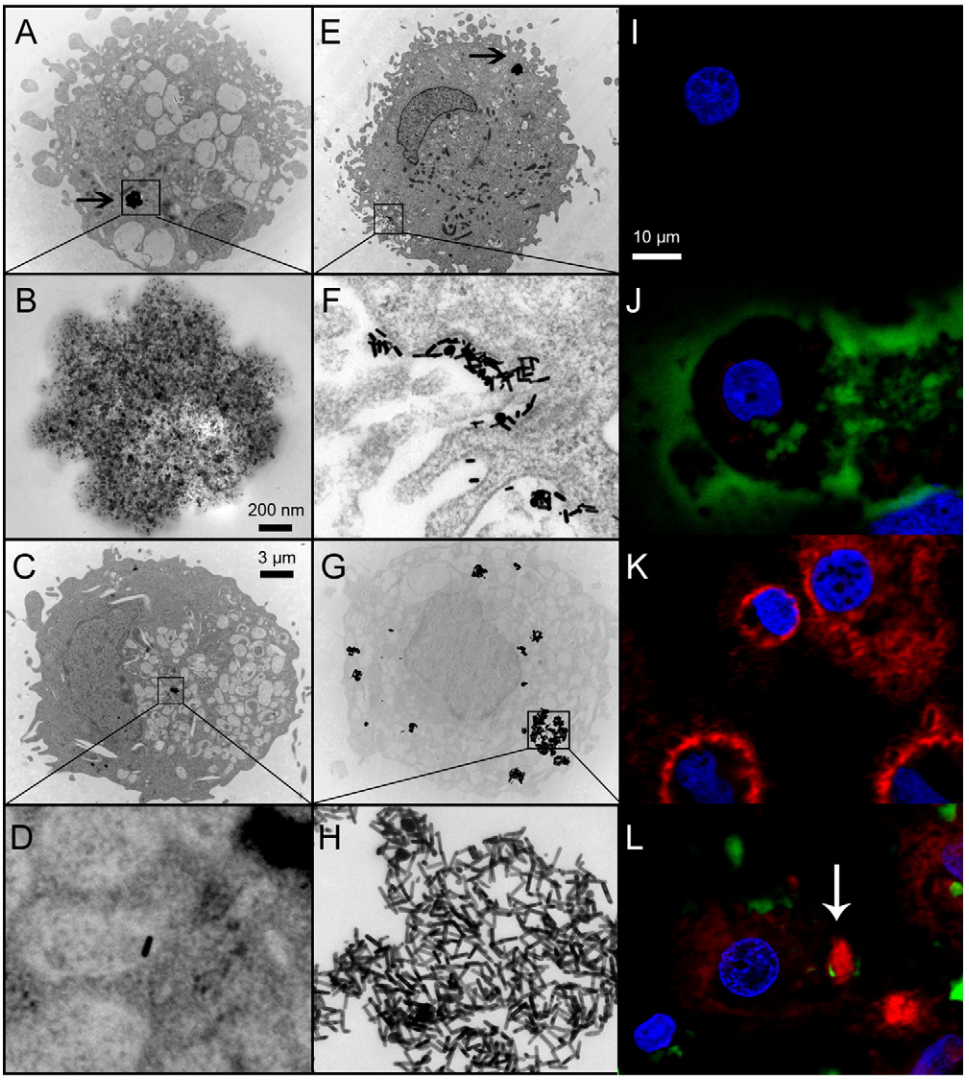

Figure 3. NP distribution in DCs and MΦ. TEM after 60 mins of culture with CTAB-coated AuNRs: mature DCs **(A,E)**, intercellular black spots **(B)** and during the attachment to the cells **(F)**. Arrows in **A** and **E** pointing at debris. Immature dendritic cells **(C)** and MΦ **(G)**, intact nanorods in immature DC **(D)** and accumulations of intact particles in MΦ **(H)**. Confocal microscopy of MΦ **(I,J)** and mature DCs **(K,L)** stained for MHC-II (anti-HLA-DR, *red*) and nuclei (DAPI, *blue*) without **(I,K)** and with **(J,L)** fluorescent NPs (*green*). The arrow in **(L)** points at NPs co-localized in the MHC-II compartment.

cells immobilized the largest quantities of gold, followed by immature DC (Figure 2).

In summary, these data provide clear evidence that the uptake of NPs is both charge dependent as well as cell-type dependent.

To study the intracellular distribution of NPs in MΦ and mature DC in more detail, TEM studies were performed. These detected marked differences in the subcellular distribution between MΦ and mature DC, specifically, a concentration in spot-like areas in mature DC but not in MΦ. Interestingly, the areas of nanorod concentration that were observed in mature DC mostly did not consist of intact NRs but of black debris (Figure 3, *A*, *B*). The debris was not an artifact due to the section preparation as only osmium was used for cell preparation for TEM studies. In immature DC, intact NRs were found inside the cell (Figure 3, *C*, *D*), similar to MΦ. In contrast to immature DC and and MΦ, intact NRs were found only during their initial attachment at the cell surface of mature DC (Figure 3, *E*, *F*). Particle accumulation in MΦ that occurred during long-term culture with amine terminated PEG rods consisted of intact NRs (Figure 3, *G*, *H*).

To address the question whether the accumulation of NPs in distinct spots in mature DC is particle-specific, we used commercial silica-based fluorescent NPs and incubated MΦ and mature DC with these particles and further stained for nuclei and MHC-II. We found that also these NPs were widely distributed in MΦ (Figure 2, *J*) whereas they accumulated in distinct spots in mature DC (Figure 2, *L*). Double-staining experiments of seedless deposition and MHC-II immunofluorescence confirmed that the NP-spot accumulation in mature DC co-localized with the MHC-II processing compartment in DC but not in MΦ (Supplementary Information Figures S2 and S3).

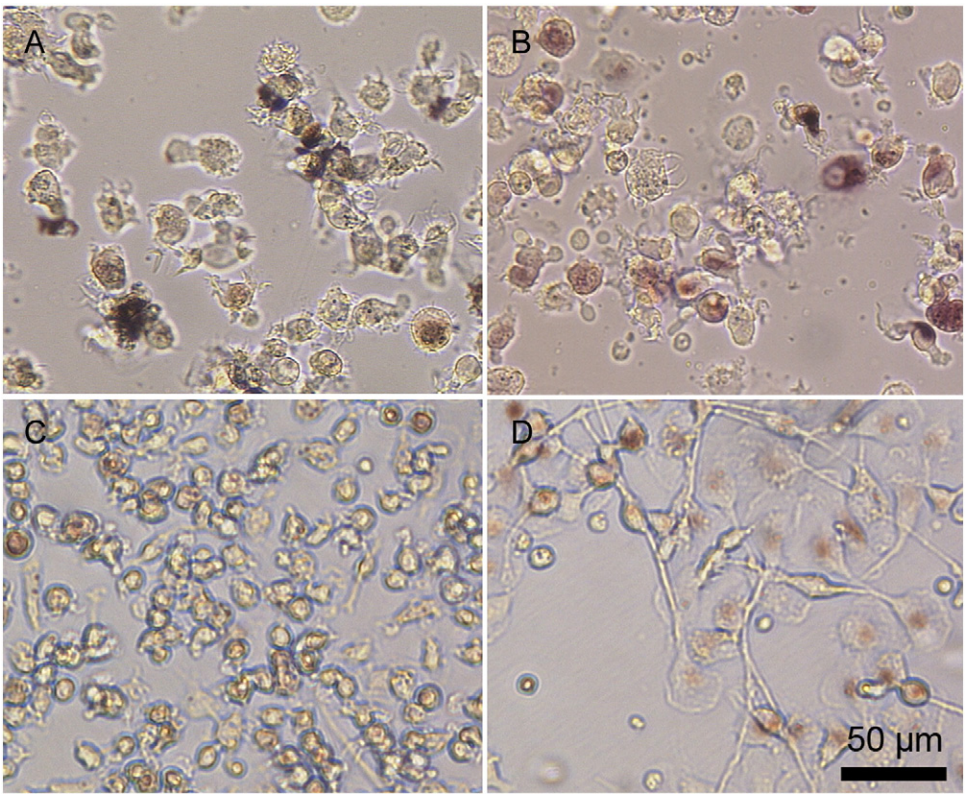

Figure 4. Effects of particle charge on the morphology of DCs and MΦ after long-term culture. Photographs of cells cultures: PEG-COOH AuNR in DC appear as black spots **(A)**, PEG-NH_2 AuNR in DC as red spots **(B)**. PEG-COOH AuNR in MΦ **(C)** and PEG-NH_2 AuNR in MΦ, visible as red area **(D)**. Bar in **D** also accounts for **A**, **B**, and **C**.

To examine additional factors that might influence the NP uptake and cellular distribution, we investigated the effect of serum proteins, bacterial products, and glucocorticoids on the uptake of NPs by human monocytes, MΦ, and DCs. We found that commercial serum free medium enhanced the uptake of negatively charged AuNPs and that both LPS and the glucocorticoid dexamethasone decreased the uptake by MΦ (Supplementary Information Figure S4).

Influence of nanorod charge and bound peptides on DC and Mφ phenotype

We have recently shown that coating of AuNRs with PEG prevents their uptake by phagocytes for at least 24 hours.[9] A functionalization of such nanorods with GLF was expected to bind to and consequently induce uptake by phagocytes.[19] Yet, neither the RGD nor the GLF peptide modification of NRs induced any observable binding to the cell surface or uptake by MΦ in short-term culture (data not shown). We therefore addressed the question whether long-term culture with different NPs and charges, respectively, and surface-bound peptides had an effect on the phenotype of DC and MΦ.

Morphological analyses of cell culture after 48 hours showed that in DCs, PEG-OH capped AuNR, in a fashion similar to that of PEG-COOH and CTAB rods, mostly resulted in black intracellular particle inclusions (Figure 4, *A*). Amine terminated NRs in most cases led to red inclusions in DC (Figure 4, *B*), similar to RGD- and GLF-capped NRs. In MΦ, PEG-OH, in a fashion similar to that of PEG-COOH NRs, were detectable as red or brown inclusions (Figure 4, *C*, *D*).

Flow cytometric studies of the effects of NPs charge and peptides on DC and MΦ surface markers showed that the molecules investigated were significantly altered in DC but not in MΦ. The peptide-modified NRs decreased the number of CD1a-expressing cells, whereas all hydroxy, amine, and carboxy endgroups increased the number of CD83-expressing DC (Figure 5).

As we found that the maturation of DC was strongly affected by the OH, NH_2, and COOH-terminated NPs, we further studied the DC activation molecules CD80, CD86, HLA-DR (MHC class II), and CD14. It appeared that the enhancement of DC maturation as induced by NP charge also resulted in a decrease in the number of cells expressing CD14, similar to the effects of cytokines used for the generation of mature DC. We found that HLA-DR, CD14, and CD80 surface expression was weakly affected by the NPs, yet the number of cells expressing CD80 and HLA-DR was weakly enhanced by amine- and carboxy-modified rods. Most interesting, both opposed charged PEG endgroups (NH_2 and COOH) significantly increased the number of cells expressing CD86 (Supplementary Information Figure S5).

Cytokine release induced in DC and MΦ by NPs

To compare the cellular responses of DC and MΦ with the different NP formulations, we investigated the release of 13

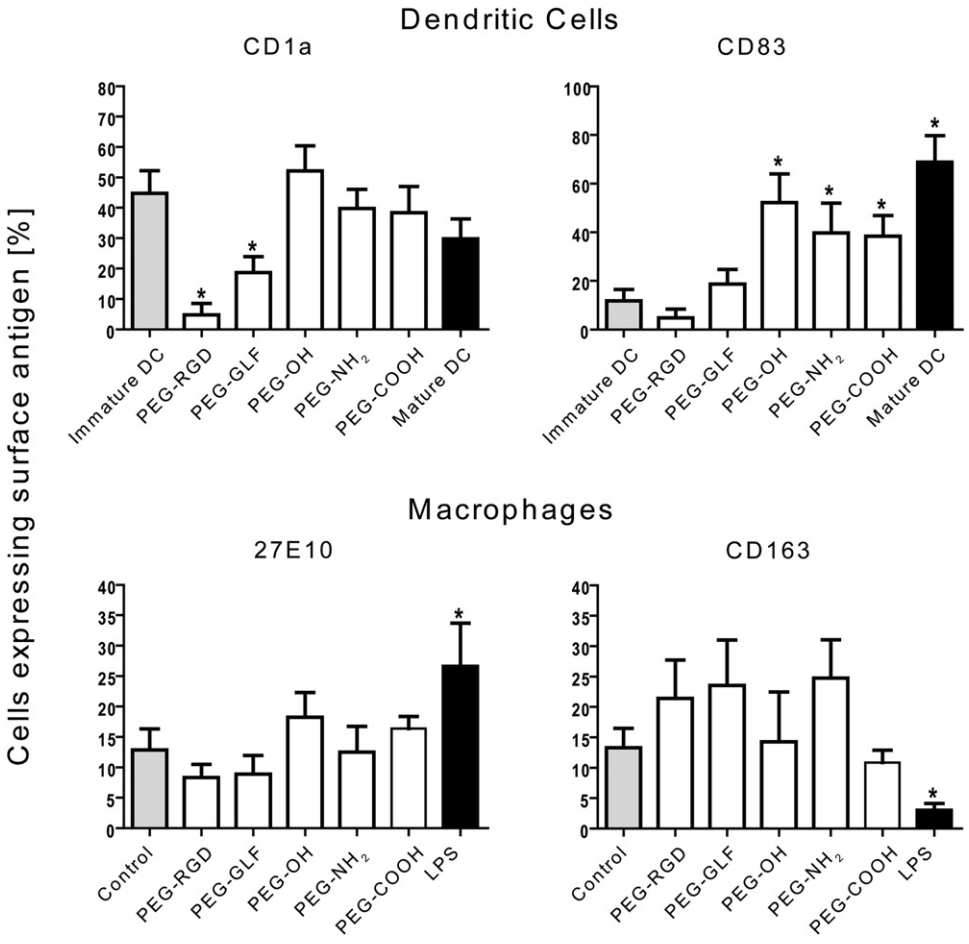

Figure 5. Flow cytometric analysis of alterations of macrophage and DC function by differently modified NRs. Statistical summary of the DC activation markers CD1a and CD83 and the macrophage function-associated molecules 27E10 (pro-inflammatory) and CD163 (anti-inflammatory) after 2 days of culture with different NRs. $^{*}P < 0.05$. Data represent mean values and SD ($n = 4$).

different cytokines and chemokines into the cell culture supernatant. LPS treatment served as positive control for cytokine release. The results of selected cytokine and chemokines are displayed in Figure 6. It was found that all NR modifications stimulated the release of the chemokine (C-C motif) ligand 2 (CCL2, MCP-1) in MΦ, but only PEG-OH-capped particles triggered its release in DC. The release profiles of CCL3 (MIP1α) and CCL4 (MIP1β) was similar to that of CCL2 (Supplementary Information Figure S6). The secretion of the monokine-induced by gamma interferon (MIG, CXCL9) was also induced in MΦ only, but interestingly was inhibited in DC. The release of IL8 (CXCL8) was found to be triggered by CTAB, as well as NH_2 and GLF capped NRs in DC, in MΦ, however, by CTAB-NRs only. IL1β secretion was found to be affected only in DC. It is notable that coupling of the peptide GLF strongly enhanced IL1β release, whereas RGD significantly inhibited it in DC. Furthermore, the release of interleukin 6 (IL6) was only stimulated in DC but not in MΦ. The release of TNFα in DC was unaffected by all types of NRs, but was stimulated by both peptide-bound NRs in MΦ. IL10 was not triggered by NPs, neither in DC, nor in MΦ (Supplementary Information Figure S6). IL2, IL4, IL5, G-CSF, TNFβ, IL12, IFNγ were not detected in cell culture supernatants.

In summary, these data show that the NPs affected the cytokine release depending on surface charge and the type of peptides bound, but apparently, also in a cell-type-dependent manner.

Discussion

The number of nanomaterial-based medical applications is rising rapidly and thus, the need for comprehensive studies facing the side effects of nano tools is more important than ever. Because most nanotherapeutics come into contact with many different RES cells in blood as well in most organs during in vivo applications,[24] we here investigated the effects of NPs with different surface charges on their uptake by different cells. Our data clearly show that all RES cell types studied take up NPs, however, with profound differences regarding the portion of ingesting cells, the amount of ingested particles and their intracelluar distribution. Apparently, the charge of NPs controls their short-term uptake by different cells of the RES, whereas

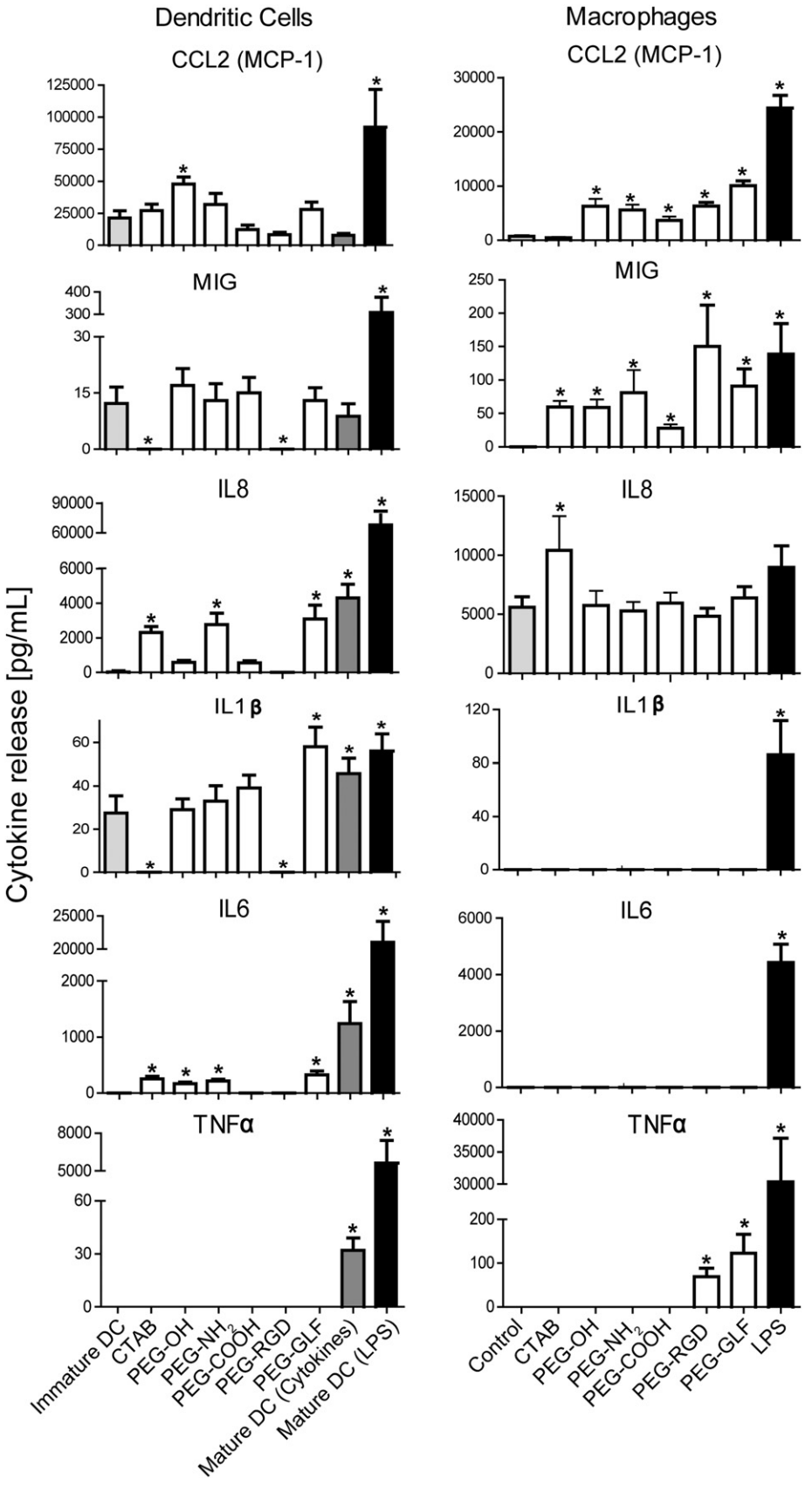

Figure 6. Effects of NR-attached peptides and charged endgroups on cytokine release by DCs and MΦ after 2 days of incubation with the NPs. *$P < 0.05$ indicates a significant difference in comparison with immature DC or to untreated MΦ, respectively. Data represent mean values and DC ($n = 4$).

coupled peptides and functional endgroups exhibit specific effects on DC and MΦ as indicated by surface marker expression and cytokine profiles.

We found it interesting that an intracellular NP accumulation in distinct areas of the MHC II compartment was observed in mature DC for the first time. MΦ and DC strongly differ in their uptake and subcellular distribution of NPs although they originate from the same progenitor cell, the monocyte. A similar mechanism based on macropinocytosis has been reported to be responsible for the uptake of large dextrane particles.[25] Though NP concentration in mature DC has not been reported before, in the 1990s it was shown that after 48 hours, the maturation of DC results in a strong reduction of the MHC II processing compartment to a distinct spot.[25] Therefore, a co-translocation of the particles into the MCH II-processing compartment accompanied with specific effects on DC maturation might be the reason for the promotion of DC maturation by NPs.[10,26]

Notably, mature DC appear to degrade NRs based on a process that has not been observed before. Therefore, we hypothesize that specific activities of serine proteases that are known to be active in DCs[12-14] might alter the shape of CTAB-stabilized NPs. Another remarkable finding was the fact that the EC ingested NPs even more efficiently than MΦ did, similar to a higher intake in comparison with human breast cancer cells.[27] Yet, it has been described that HUVEC, which are abundant in the body, might be damaged by particle uptake,[28] whereas MΦ are known to scavenge protein-metal complexes such as hemoglobin[29] that might render MΦ less sensitive to particle intake in vivo. MΦ and DC potentially also affect cells of the adaptive immune system, specifically T cells.[30]

We further report an optimized method to couple peptides onto AuNRs, aiming at a cell-specific targeting and thereby an increased intake by MΦ. However, we did not observe such an induction in MΦ by the peptide GLF as reported previously.[19] Yet, we found that the uptake pf PEGylated NPs, regardless of attached peptides or functional endgroups, are taken up by all RES cells with delay, as is similar to recent findings.[9]

The finding that the various NP formulations differently affect the expression of marker molecules relevant for cell activation emphasizes a RES-cell specific response to NPs. Others have shown that NPs can both enhance DC functions[10] or that polymeric fluorescent preserve the functions of DCs.[31] Our data show that NP-coupled peptides inhibit DC maturation reflected by a decreased expression of CD1a and CD83 and that NP-coupled charged endgroups induce a more rapid and significant alteration of DC phenotype. These changes were notably more rapid than those of MΦ that occur as late as after 7 days.[9]

It is interesting that, as with amine terminated PEG endgroups,[9] both coupled peptides used in this study induced the expression of CD163, a scavenger receptor that is among others involved in hemoglobin clearance and, thus, in iron homeostasis.[32] Interestingly, others have shown that diesel-exhaust particles interact with DC via scavenger receptors.[33] Therefore, CD163 expression might be triggered similarly by cell-metal-protein-complex interactions, and it can be hypothesized that the biological function of CD163 expression might aim at neutralizing potential antioxidant activities of metal-associated complexes.

The release of CCL2, which is involved in the recruitment of monocytes,[34] was similar to that of the cognate T-cell-attracting chemokines CCL3 and CCL4.[35] Moreover, the biologically active peptides RGD and GLF elicit a different cytokine pattern in DC and MΦ and remarkably, RGD appears to exert opposite effects in cytokine release in DC in comparison with MΦ, specifically an inhibition of MIG in DC and a stimulation in MΦ. MIG is also involved in T-cell trafficking.[36] IL8 was both in DC and MΦ induced by CTAB-capped NRs, and in DC, additionally, by NH_2- and GLF-terminated particles. This chemokine is known to be mainly involved in attracting neutrophils.[37]

In contrast to the RGD sequence, GLF appears to induce cytokine release in DC as well as in MΦ that might be led back to its immunostimulating functions.[19] NP-bound peptides affect macrophage response after as early as 48 hours, differing from the delayed change in macrophage phenotype by PEG-coupled functional endgroups.[9] The studied peptides significantly induced release of the pro-inflammatory cytokine TNFα and of MIG in MΦ after only 48 hours.

In conclusion, our data show that all cells of the RES are able to internalize AuNPs. The uptake is dependent on the surface charge, time, and cell type but cannot be accelerated using surface-bound biologically active peptides RGD and GLF. Interestingly, the subcellular distribution of NPs differs in MΦ and DCs. Furthermore, NPs in long-term culture influence the inflammatory functions of DC and MΦ depending on NP surface charge, and the cell type that interacts with the particles. The inflammatory potency can be modulated by NR-coupled peptides and functional endgroups in a cell-type dependent manner. Our studies highlight the importance of monocyte-derived cells in host-NP interactions and provide new insights into the effects of NP charge and coupled peptides on DC and MΦ functions. Assessing the overall effects of NPs on immune-cell activation and function requires further studies using in vivo approaches.

Acknowledgments

TEM was performed at Electron Microscopic Facility (EMF), University Hospital, RWTH Aachen. The authors thank Bender Medsystems for assistance with cytokine measurement and are grateful to Gerhard Müller-Newen, Institute of Biochemistry and Molecular Biology, RWTH Aachen, Germany, for help with confocal microscopy.

Appendix A. Supplementary data

Supplementary data to this article can be found online at doi:10.1016/j.nano.2012.02.012.

References

1. Tong L, Wei Q, Wei A, Cheng JX. Gold nanorods as contrast agents for biological imaging: optical properties, surface conjugation and photothermal effects. *Photochem Photobiol* 2009;**85**:21-32.
2. Huff TB, Tong L, Zhao Y, Hansen MN, Cheng JX, Wei A. Hyperthermic effects of gold nanorods on tumor cells. *Nanomedicine (Lond)* 2007;**2**:125-32.

3. Gref R, Luck M, Quellec P, Marchand M, Dellacherie E, Harnisch S, et al. 'Stealth' corona-core nanoparticles surface modified by polyethylene glycol (PEG): influences of the corona (PEG chain length and surface density) and of the core composition on phagocytic uptake and plasma protein adsorption. *Colloids Surf B Biointerfaces* 2000;**18**: 301-13.
4. Maeda H. Tumor-selective delivery of macromolecular drugs via the EPR effect: background and future prospects. *Bioconjug Chem* 2010;**21**: 797-802.
5. Holback H, Yeo Y. Intratumoral drug delivery with nanoparticulate carriers. *Pharm Res* 2011.
6. Huang X, Peng X, Wang Y, Shin DM, El-Sayed MA, Nie S. A reexamination of active and passive tumor targeting by using rod-shaped gold nanocrystals and covalently conjugated peptide ligands. *ACS Nano* 2010;**4**:5887-96.
7. Tagalakis AD, Grosse SM, Meng QH, Mustapa MF, Kwok A, Salehi SE, et al. Integrin-targeted nanocomplexes for tumour specific delivery and therapy by systemic administration. *Biomaterials* 2011;**32**:1370-6.
8. Eghtedari M, Liopo AV, Copland JA, Oraevsky AA, Motamedi M. Engineering of hetero-functional gold nanorods for the in vivo molecular targeting of breast cancer cells. *Nano Lett* 2009;**9**:287-91.
9. Bartneck M, Keul HA, Singh S, Czaja K, Bornemann J, Bockstaller M, et al. Rapid uptake of gold nanorods by primary human blood phagocytes and immunomodulatory effects of surface chemistry. *ACS Nano* 2010;**4**:3073-86.
10. Clawson C, Huang CT, Futalan D, Martin Seible D, Saenz R, Larsson M, et al. Delivery of a peptide via poly(D,L-lactic-co-glycolic) acid nanoparticles enhances its dendritic cell-stimulatory capacity. *Nanomedicine* 2010;**6**:651-61.
11. Steinbach F, Krause B, Blass S, Burmester GR, Hiepe F. Development of accessory phenotype and function during the differentiation of monocyte-derived dendritic cells. *Res Immunol* 1998;**149**:627-32.
12. Delamarre L, Pack M, Chang H, Mellman I, Trombetta ES. Differential lysosomal proteolysis in antigen-presenting cells determines antigen fate. *Science* 2005;**307**:1630-4.
13. Savina A, Amigorena S. Phagocytosis and antigen presentation in dendritic cells. *Immunol Rev* 2007;**219**:143-56.
14. Radzicka A, Wolfenden R. A proficient enzyme. *Science* 1995;**267**: 90-3.
15. Engel P, Tedder TF. New CD from the B cell section of the fifth international workshop on human leukocyte differentiation antigens. *Leuk Lymphoma* 1994;**13**(Suppl 1):61-4.
16. Hunger RE, Sieling PA, Ochoa MT, Sugaya M, Burdick AE, Rea TH, et al. Langerhans cells utilize CD1a and langerin to efficiently present nonpeptide antigens to T cells. *J Clin Invest* 2004;**113**:701-8.
17. Palucka KA, Taquet N, Sanchez-Chapuis F, Gluckman JC. Dendritic cells as the terminal stage of monocyte differentiation. *J Immunol* 1998; **160**:4587-95.
18. Wright SD, Ramos RA, Tobias PS, Ulevitch RJ, Mathison JC. CD14, a receptor for complexes of lipopolysaccharide (LPS) and LPS binding protein. *Science* 1990;**249**:1431-3.
19. Jaziri M, Migliore-Samour D, Casabianca-Pignede MR, Keddad K, Morgat JL, Jolles P. Specific binding sites on human phagocytic blood cells for Gly-Leu-Phe and Val-Glu-Pro-Ile-Pro-Tyr, immunostimulating peptides from human milk proteins. *Biochim Biophys Acta* 1992;**1160**: 251-61.
20. Nikoobakht B, El-Sayed MA. Preparation and growth mechanism of gold nanorods (NRs) using seed-mediated growth method. *Chem Mater* 2003;**15**:1957-62.
21. Gimbrone Jr MA, Cotran RS, Folkman J. Human vascular endothelial cells in culture. Growth and DNA synthesis. *J Cell Biol* 1974;**60**:673-84.
22. Jonuleit H, Kuhn U, Muller G, Steinbrink K, Paragnik L, Schmitt E, et al. Pro-inflammatory cytokines and prostaglandins induce maturation of potent immunostimulatory dendritic cells under fetal calf serum-free conditions. *Eur J Immunol* 1997;**27**:3135-42.
23. Jacobs JJ, Lehe CL, Hasegawa H, Elliott GR, Das PK. Skin irritants and contact sensitizers induce Langerhans cell migration and maturation at irritant concentration. *Exp Dermatol* 2006;**15**:432-40.
24. Sadauskas E, Wallin H, Stoltenberg M, Vogel U, Doering P, Larsen A, et al. Kupffer cells are central in the removal of nanoparticles from the organism. *Part Fibre Toxicol* 2007;**4**:10.
25. Sallusto F, Cella M, Danieli C, Lanzavecchia A. Dendritic cells use macropinocytosis and the mannose receptor to concentrate macromolecules in the major histocompatibility complex class II compartment: downregulation by cytokines and bacterial products. *J Exp Med* 1995; **182**:389-400.
26. Koike E, Takano H, Inoue K, Yanagisawa R, Kobayashi T. Carbon black nanoparticles promote the maturation and function of mouse bone marrow-derived dendritic cells. *Chemosphere* 2008;**73**:371-6.
27. Osaka T, Nakanishi T, Shanmugam S, Takahama S, Zhang H. Effect of surface charge of magnetite nanoparticles on their internalization into breast cancer and umbilical vein endothelial cells. *Colloids Surf B Biointerfaces* 2009;**71**:325-30.
28. Langeggen H, Namork E, Johnson E, Hetland G. HUVEC take up opsonized zymosan particles and secrete cytokines IL-6 and IL-8 in vitro. *FEMS Immunol Med Microbiol* 2003;**36**:55-61.
29. Mosser DM, Edwards JP. Exploring the full spectrum of macrophage activation. *Nat Rev Immunol* 2008;**8**:958-69.
30. Kawai J, Inaba K, Komatsubara S, Hirayama Y, Naito K, Muramatsu S. Role of macrophages as modulators but not as autonomous accessory cells in the proliferative response of immune T cells to soluble antigen. *Cell Immunol* 1987;**109**:1-11.
31. Zupke O, Distler E, Baumann D, Strand D, Meyer RG, Landfester K, et al. Preservation of dendritic cell function upon labeling with amino functionalized polymeric nanoparticles. *Biomaterials* 2010;**31**: 7086-95.
32. Vallelian F, Schaer CA, Kaempfer T, Gehrig P, Duerst E, Schoedon G, et al. Glucocorticoid treatment skews human monocyte differentiation into a hemoglobin-clearance phenotype with enhanced heme-iron recycling and antioxidant capacity. *Blood* 2010;**116**:5347-56.
33. Taront S, Dieudonne A, Blanchard S, Jeannin P, Lassalle P, Delneste Y, et al. Implication of scavenger receptors in the interactions between diesel exhaust particles and immature or mature dendritic cells. *Part Fibre Toxicol* 2009;**6**:9.
34. Melgarejo E, Medina MA, Sanchez-Jimenez F, Urdiales JL. Monocyte chemoattractant protein-1: a key mediator in inflammatory processes. *Int J Biochem Cell Biol* 2009;**41**:998-1001.
35. Castellino F, Huang AY, Altan-Bonnet G, Stoll S, Scheinecker C, Germain RN. Chemokines enhance immunity by guiding naive CD8+ T cells to sites of CD4+ T cell-dendritic cell interaction. *Nature* 2006;**440**: 890-5.
36. Kryczek I, Banerjee M, Cheng P, Vatan L, Szeliga W, Wei S, et al. Phenotype, distribution, generation, and functional and clinical relevance of Th17 cells in the human tumor environments. *Blood* 2009;**114**:1141-9.
37. Martin D, Galisteo R, Gutkind JS. CXCL8/IL8 stimulates vascular endothelial growth factor (VEGF) expression and the autocrine activation of VEGFR2 in endothelial cells by activating NFkappaB through the CBM (Carma3/Bcl10/Malt1) complex. *J Biol Chem* 2009;**284**:6038-42.